ChemComm

COMMUNICATION

View Article Online
View Journal | View Issue

Cite this: *Chem. Commun.*, 2014, **50**, 945

Received 23rd August 2013,
Accepted 27th November 2013

DOI: 10.1039/c3cc46456c

www.rsc.org/chemcomm

Hydrogenase biomimetics: $Fe_2(CO)_4(\mu\text{-dppf})(\mu\text{-pdt})$ (dppf = 1,1′-bis(diphenylphosphino)ferrocene) both a proton-reduction and hydrogen oxidation catalyst†

Shishir Ghosh,[a] Graeme Hogarth,*[ab] Nathan Hollingsworth,[a] Katherine B. Holt,*[a] Shariff E. Kabir[c] and Ben E. Sanchez[a]

$Fe_2(CO)_4(\mu\text{-dppf})(\mu\text{-pdt})$ catalyses the conversion of protons and electrons into hydrogen and also the reverse reaction thus mimicking both types of binuclear hydrogenase enzymes.

Hydrogenases are enzymes capable of reversibly converting protons and electrons into hydrogen[1] and over the past two decades their active sites have been discerned primarily from crystallographic studies,[2–4] with three phylogenetically different enzyme types being identified. The two most widely studied of these are the so-called [FeFe]H_2ase and [NiFe]H_2ase enzymes (Chart 1) the active sites of which contain two transition metal atoms. While both enzyme types are able to catalyse both the reduction of protons and oxidation of hydrogen, [FeFe]H_2ase enzymes are more efficient with respect to the former, while [NiFe]H_2ase enzymes are favoured for the oxidation of hydrogen.[5]

Over the past 15 years, a range of structural and functional biomimetics of the active sites of these enzymes have studied[5,6] with key insights into the likely mechanism(s) being determined[7] and recently some impressive turnovers for the electrocatalytic reduction of protons being reported.[8] However, as far as we are aware, no biomimetic has yet been shown to both be catalytic for the reduction of protons and electrons to hydrogen and also the oxidation of hydrogen to protons and electrons.[9] We herein describe $Fe_2(CO)_4(\mu\text{-dppf})(\mu\text{-pdt})$ (**2**) {pdt = $S(CH_2)_3S$, dppf = 1,1′-bis(diphenylphosphino)ferrocene} which we have shown is a catalyst for both of these transformations.

Heating a toluene solution of equimolar amounts of $Fe_2(CO)_6(\mu\text{-pdt})$ (**1**) with dppf initially leads to formation of the linked tetranuclear complex $\{Fe_2(CO)_5(\mu\text{-pdt})\}_2(\mu,\kappa^1,\kappa^1\text{-dppf})$[10] and unreacted dppf, which slowly rearranges to afford $Fe_2(CO)_4(\mu\text{-dppf})(\mu\text{-pdt})$ (**2**) in moderate yields‡ as an air-stable orange solid (Scheme 1) being characterised by analytical and spectroscopic data together with a single-crystal X-ray diffraction study, the results of which are summarised in Fig. 1. The molecule is as expected and bond lengths and angles are generally within the ranges of those seen in related complexes.[10,11] The iron–iron bond length of 2.6133(6) Å is, however, some 0.1 Å longer than is generally the case[10–12] suggesting that the flexible nature of the dppf ligand allows this bond to relax. The non-bonding iron–iron distances of 4.581 and 4.613 Å suggest that there is no direct contact between the two redox centres in the molecule.

Cyclic voltammograms (CVs) of **2** were recorded in acetonitrile at various scan rates as shown in Fig. 2. The complex undergoes an electrochemically reversible oxidation at $E_{1/2}$ = 0.05 V (ΔE = 60 mV) and a further reversible oxidation at $E_{1/2}$ = 0.685 V (ΔE = 70 mV). The former is associated with oxidation of the diiron centre and the latter most likely with the ferrocene moiety (see later). The reversibility of both oxidative processes is maintained at all scan rates. The complex also shows two overlapping irreversible reduction peaks at E_p = −2.10 V and E_p = −2.19 V which become separated at higher scan rates ($\geq$0.25 V s^{-1}) (Fig. 2). Two small oxidation peaks are also

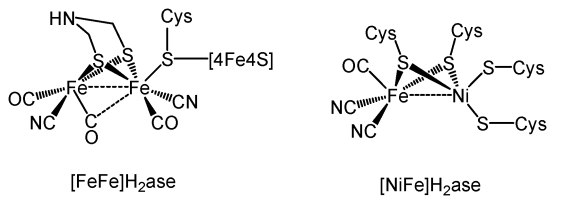

Chart 1 Structure of the active site of [FeFe]H_2ase and [NiFe]H_2ase.

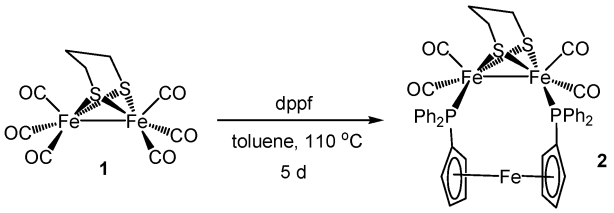

Scheme 1 Preparation of $Fe_2(CO)_4(\mu\text{-dppf})(\mu\text{-pdt})$ (**2**).

[a] *Department of Chemistry, University College London, 20 Gordon Street, London, WC1H 0AJ, UK. E-mail: g.hogarth@ucl.ac.uk*
[b] *Department of Chemistry, King's College London, Britannia House, 7 Trinity Street, London SE1 1DB, UK. E-mail: Graeme.hogarth@kcl.ac.uk*
[c] *Department of Chemistry, Jahangirnagar University, Savar, Dhaka 1342, Bangladesh*

† Electronic supplementary information (ESI) available: Experimental details, crystallographic data. CCDC 956914. For ESI and crystallographic data in CIF or other electronic format see DOI: 10.1039/c3cc46456c

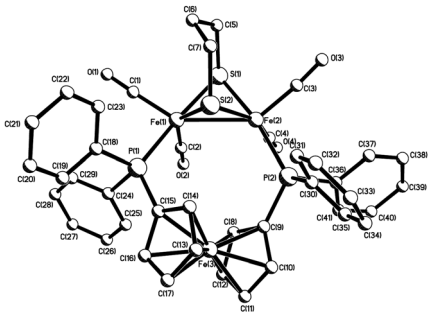

Fig. 1 Molecular structure of **2**. Selected bond lengths [Å] and bond angles [°]: Fe(1)–Fe(2) 2.6133(6), Fe(1)–P(1) 2.2256(6), Fe(2)–P(2) 2.2679(6), P(1)–Fe(1)–S(1) 174.34(2), P(2)–Fe(2)–S(1) 167.79(2).

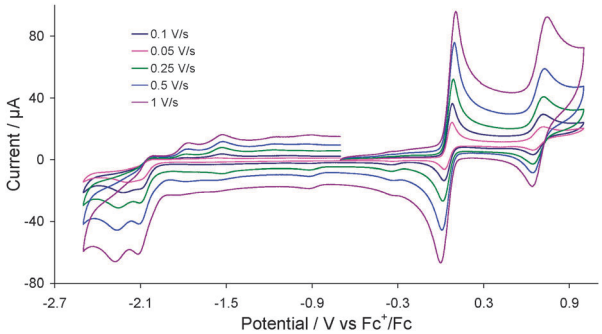

Fig. 2 CVs of **2** in MeCN (1 mM solution, supporting electrolyte $[NBu_4][PF_6]$, glassy carbon electrode, potential *vs.* Fc^+/Fc) at various scan rates.

observed at $E_p = -1.80$ V and $E_p = -1.53$ V on the return scan being due to the product formed in the reductive processes, whilst the small reduction peak appeared at $E_p = -0.35$ V on the return scan is associated with the first oxidation product.

Upon chemical oxidation, by addition of $FcPF_6$ to a CH_2Cl_2 solution of **2**, new IR absorption bands appear at 2044 and 2013 cm^{-1} (Fig. S1, ESI†). The 60 cm^{-1} shift of the first ν_{CO} band to higher energy is indicative of oxidation of the diiron centre allowing assignment of the couple at 0.05 V *vs.* Fc^+/Fc to this process. The second oxidation we believe is associated with the dppf ligand. Uncoordinated dppf undergoes an irreversible oxidation at 0.20 V which becomes reversible and shifts to more positive potentials upon coordination to a metal centre.[13] The relative position of the second oxidative process *vs.* Fc^+/Fc and its chemical reversibility is consistent with the $Fe^{II/III}$ couple of the ferrocene moiety.

We next assessed the ability of **2** to bind a proton. Addition of one molar equivalent of $HBF_4{\cdot}Et_2O$ to a CH_2Cl_2 solution of **2** (or two to an MeCN solution) resulted in the rapid and clean formation of the cationic-hydride $[Fe_2(CO)_4(\mu\text{-H})(\mu\text{-dppf})(\mu\text{-pdt})][BF_4]$ (**3**).‡ Further, and unlike most related cationic complexes,[11] addition of base leads to regeneration of the neutral complex. This suggests that while **2** is able to bind a proton, it is relatively weakly held. Related $Fe_2(CO)_4(\mu$-diphosphine$)(\mu$-dithiolate) complexes do not generally form stable cationic hydrides, the exceptions being $Fe_2(CO)_4(\mu\text{-}Cy_2PCH_2PCy_2)(\mu\text{-pdt})$ and $Fe_2(CO)_4\{\mu\text{-}Ph_2P(CH_2)_4PPh_2\}(\mu\text{-pdt})$ containing basic and flexible diphosphines respectively.[11] Thus, the greater flexibility of dppf in **2** appears to be the reason for its ability to bind a proton.

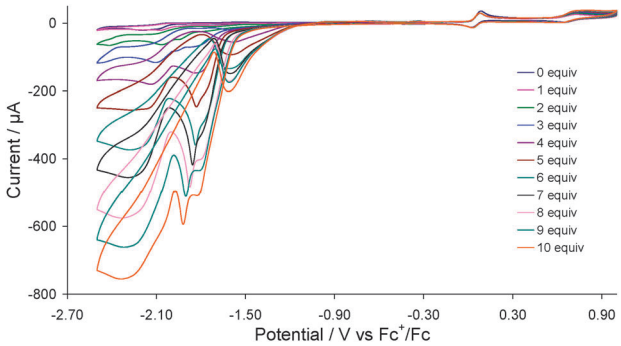

Fig. 3 CVs of **2** in the absence and presence of 1–10 molar equivalents of $HBF_4{\cdot}Et_2O$ (1 mM solution in MeCN, supporting electrolyte $[NBu_4][PF_6]$, scan rate 0.1 V s^{-1}, glassy carbon electrode, potential *vs.* Fc^+/Fc).

Complex **2** was first tested as a proton reduction catalyst in the presence of $HBF_4{\cdot}Et_2O$ in MeCN. Fig. 3 shows the CVs upon addition of between 1–10 equivalents of acid. A new reduction wave appears at $E_p = -1.70$ V upon addition of acid being associated with reduction of **3**, its height growing with increasing amounts of acid, being characteristic of electrocatalytic proton reduction.[6] At higher amounts of acid ($\geq$7 molar equivalents) this wave splits into two distinct peaks possibly resulting from reduction of the putative cation $[HFe_2(CO)_4(\mu\text{-H})(\mu\text{-dppf})(\mu\text{-pdt})]^+$ (see below). Another catalytic wave is also observed at $E_p = -2.10$ V which competes with the direct reduction of $HBF_4{\cdot}Et_2O$ by the glassy carbon electrode as this electrode becomes catalytically active beyond -2.00 V in presence of strong acids.[14] On the return scan a further catalytic wave is seen at $E_p = -1.55$ V implying that the species responsible for the first catalytic wave is regenerated. Thus it appears that **2** enters into the catalytic cycle *via* a CE mechanism to generate the neutral paramagnetic complex $Fe_2(CO)_4(\mu\text{-H})(\mu\text{-dppf})(\mu\text{-pdt})$[15] which either protonates or undergoes a further reduction before second protonation to liberate hydrogen. The peak heights of the oxidative processes do not change during the experiment showing the robustness of **2** under the operating conditions.

Recent developments in hydrogenase biomimics suggest that H_2 activation can be favoured by the presence of a mild and chemically inert oxidant in the diiron models.[16] The concept was recently experimentally implemented by Camara and Rauchfuss[17,18] who utilised $(C_5Me_5)Fe(C_5Me_4)CH_2PEt_2$ (FcP*) as the intramolecular oxidant, the $Fe^{II/III}$ couple ($E_{1/2} = -0.59$ V) of which lies closer to the H_2/H^+ couple *vs.* the Fc^+/Fc couple.[18] They showed that the dication of $Fe_2(CO)_3(\kappa^2\text{-}Ph_2PCH{=}CHPPh_2)(\kappa^1\text{-FcP*})\{\mu\text{-}SCH_2N(Bz)CH_2S\}$ (**A**) cleaves H_2, being facilitated by an intramolecular electron-transfer in its doubly oxidised state, the electron transferring from the diiron unit to the pendent FcP* ligand *i.e.* switching from Fe(III)Fe(II)Fe(I) to Fe(II)Fe(II)Fe(II).[18] In contrast, an analogue of **A** in which FcP* is replaced by PMe_3 is catalytically inactive towards H_2 oxidation.[18] That there is electronic communication between the diiron core and the ferrocene in **A** despite the presence of a methylene linker unit prompted us to investigate the possibility of electronic communication between the two redox-active metal centres in **2**. Indeed we found that **2** catalytically cleaves H_2 in presence of a base (pyridine) in its 2^{2+} state (Fig. 4). Thus, addition of equimolar amount of pyridine to an acetonitrile solution of **2**

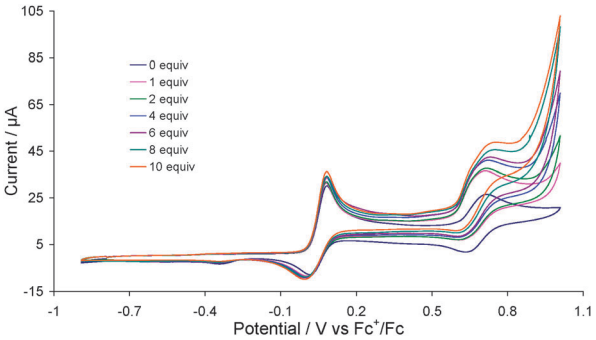

Fig. 4 CVs of **2** in the absence of pyridine and in the presence of varying molar equivalents of pyridine under a H_2 atmosphere (1 mM solution in MeCN, supporting electrolyte $[NBu_4][PF_6]$, scan rate 0.1 V s^{-1}, glassy carbon electrode, potential *vs.* Fc^+/Fc).

under H_2 results in an increase of the oxidative peak current of the second oxidation process of **2** by 10 μA, which reaches 22 μA upon addition of 10 equivalents of pyridine. No such catalytic wave was observed when the same experiment was carried out in absence of base (Fig. S5, ESI†) or H_2 (Fig. S6, ESI†). Similarly $Fe_2(CO)_4(\mu\text{-}Ph_2PCH_2PPh_2)(\mu\text{-pdt})$[11] does not show catalytic waves under the same conditions even when ferrocene is added. At this stage we do not have a clear view of the likely mechanism operating. It has been proposed[18] and examined theoretically[19] that $\mathbf{A}^{2+}$ heterolytically cleaves H_2 to afford a terminal hydride and nitrogen-bound proton. This clearly cannot occur in the case of **2** and thus we tentatively propose the intermediate formation of a cationic dihydride.

In summary we have shown that a biomimetic of the diiron hydrogenase can catalyse both the reduction of protons and H_2 oxidation. We are currently developing a range of related biomimetics containing different secondary redox-active centres[20] and using density functional theory calculations in order to more fully understand the electronic structure of $\mathbf{2}^{2+}$ and the nature of the H_2 oxidation process.

We are grateful to the Commonwealth Scholarship Commission for the award of a Commonwealth Scholarship to S.G. and the EPSRC for a postdoctoral fellowship to N.H.

Notes and references

‡ Synthesis of **2**. A mixture of **1** (0.10 g, 0.26 mmol) and dppf (0.14 g, 0.26 mmol) in toluene (100 ml) was heated at reflux for 5 d resulting in a colour change from orange to red-brown. After cooling to room temperature, volatiles were removed under reduced pressure to give a dark oily red residue. This was washed with hexanes (3 × 5 ml) and dried. Extraction into a minimum volume of dichloromethane followed by addition of hexanes and rotary evaporation gave **2** as a dry red solid (0.12 g, 52%). **2** can also be prepared upon heating a mixture of $\{Fe_2(CO)_5(\mu\text{-pdt})\}_2(\mu,\kappa^1,\kappa^1\text{-dppf})$[10] and dppf in toluene over a similar period. IR ν(CO)(CH_2Cl_2) 1986s, 1949vs, 1918s 1896w cm^{-1}. ^1H NMR ($CDCl_3$) δ 8.01 (t, J 8.2, 2H, Ph), 7.67–6.99 (m, 18H, Ph), 4.93 (brs, 2H, CH), 4.46 (s, 2H, CH), 4.44 (s, 2H, CH), 4.01 (s, 2H, CH), 2.60 (br, 2H, CH_2), 2.31 (m, 2H, CH_2), 2.13 (br, 2H, CH_2). $^{31}P\{^1H\}$NMR ($CDCl_3$) 51.3 (s) ppm. Elemental analysis calc. for $Fe_3S_2P_2O_4C_{41}H_{35}\cdot0.5CH_2Cl_2$ (found): C 54.16 (53.41), H 3.81 (3.75). X-ray data for $Fe_3S_2P_2O_4C_{41}H_{35}\cdot0.5CH_2Cl_2$: red block, dimensions 0.38 × 0.32 × 0.16 mm, triclinic, space group $P\bar{1}$, a = 9.7365(19), b = 13.149(3), c = 16.654(3) Å, α = 99.609(3), β = 94.376(3), γ = 111.343(3)°, V = 1936.1(7) $Å^3$, Z = 2, F(000) 944, $d_{calc.}$ = 1.588 g cm^{-3}, μ = 1.411 mm^{-1}. 16 800 reflections were collected, 8886 unique [R(int) = 0.0333] of which 8134 were observed [$I > 2.0\sigma(I)$]. At convergence, R_1 = 0.0345, wR_2 = 0.0911 [$I > 2.0\sigma(I)$] and R_1 = 0. 0374, wR_2 = 0.0929 (all data), for 511 parameters. CCDC number 956914. Synthesis of **3**. To a CH_2Cl_2 (50 ml) solution of **2** (0.05 g, 0.06 mmol) was added a few drops of HBF_4. The mixture was stirred at room temperature for 20 min without any noticeable change. Volatiles were removed under reduced pressure and the resulting deep red oily solid washed with a small portion of Et_2O to remove excess acid. The remaining solid was dissolved in a minimum amount of CH_2Cl_2 which was then layered with hexanes. Slow mixing of the solutions afforded **3** (0.04 g, 73%) as a dry red solid. IR ν(CO)(CH_2Cl_2) 2058s, 2040s, 2002s cm^{-1}. ^1H NMR ($CDCl_3$) δ 8.11–7.33 (m, 20H, Ph), 4.74 (s, 2H, CH), 4.68 (s, 2H, CH), 4.49 (s, 2H, CH), 4.32 (s, 2H, CH), 2.86 (br, 2H, CH_2), 2.74 (m, 2H, CH_2), 2.48 (br, 2H, CH_2), −12.40 (t, J 17.6, 1H, μ-H). $^{31}P\{^1H\}$ NMR (CD_2Cl_2) 44.8 (s) ppm.

1 M. W. W. Adams and E. I. Stiefel, *Science*, 1998, **282**, 1842–1843; R. Cammack, *Nature*, 1999, **397**, 214–215; M. Frey, *ChemBioChem*, 2002, **3**, 153–160.
2 J. W. Peters, W. N. Lanzilotta, B. J. Lemon and L. C. Seefeldt, *Science*, 1998, **282**, 1853–1858; Y. Nicolet, C. Piras, P. Legrand, C. E. Hatchikian and J. C. Fontecillacamps, *Structure*, 1999, **7**, 13–23.
3 A. Volbeda, M. H. Charon, C. Piras, C. E. Hatchikian, M. Frey and J. C. Fontecillacamps, *Nature*, 1995, **373**, 580–587.
4 S. Shima, O. Pilak, S. Vogt, M. Schick, M. S. Stagni, W. Meyer-Klaucke, E. Warkentin, R. K. Thauer and U. Ermler, *Science*, 2008, **321**, 572–575; S. Shima, E. J. Lyon, R. K. Thauer, B. Mienert and E. Bill, *J. Am. Chem. Soc.*, 2005, **127**, 10430–10435.
5 C. Tard and C. J. Pickett, *Chem. Rev.*, 2009, **109**, 2245–2274.
6 For some reviews of this area see: I. P. Georgakaki, L. M. Thomson, E. J. Lyon, M. B. Hall and M. Y. Darensbourg, *Coord. Chem. Rev.*, 2003, **238–239**, 255–266; D. J. Evans and C. J. Pickett, *Chem. Soc. Rev.*, 2003, **32**, 268–287; T. B. Rauchfuss, *Inorg. Chem.*, 2004, **43**, 14–26; L. Sun, B. Åkermark and S. Ott, *Coord. Chem. Rev.*, 2005, **249**, 1653–1663; X. Liu, S. K. Ibrahim, C. Tard and C. J. Pickett, *Coord. Chem. Rev.*, 2005, **249**, 1641–1652; J.-F. Capon, F. Gloaguen, P. Schollhammer and J. Talarmin, *Coord. Chem. Rev.*, 2005, **249**, 1664–1676.
7 C. Greco, M. Bruschi, L. D. Gioia and U. Ryde, *Inorg. Chem.*, 2007, **46**, 5911–5921; C. Greco, M. Bruschi, P. Fantucci, U. Ryde and L. De Gioia, *J. Am. Chem. Soc.*, 2011, **133**, 18742–18749; S. Trohalaki and R. Pachter, *Int. J. Hydrogen Energy*, 2010, **35**, 5318–5331.
8 S. Dey, A. Rana, S. G. Day and A. Dey, *ACS Catal.*, 2013, **3**, 429–436.
9 N. Wang, M. Wang, L. Chen and L. Sun, *Dalton Trans.*, 2013, **42**, 12059–12071.
10 X.-F. Liu and B.-S. Yin, *J. Coord. Chem.*, 2010, **63**, 4061–4067.
11 F. I. Adam, G. Hogarth, S. E. Kabir and I. Richards, *C. R. Chim.*, 2008, **11**, 890–905; F. I. Adam, G. Hogarth and I. Richards, *J. Organomet. Chem.*, 2007, **692**, 3957–3968.
12 S. Ghosh, G. Hogarth, N. Hollingsworth, K. B. Holt, I. Richard, M. G. Richmond, B. Sanchez and D. Unwin, *Dalton Trans.*, 2013, **42**, 6775–6792; F. Ridley, S. Ghosh, G. Hogarth, N. Hollingsworth, K. B. Holt and D. Unwin, *J. Electroanal. Chem.*, 2013, **703**, 14–22; G. Hogarth, S. E. Kabir and I. Richards, *Organometallics*, 2010, **29**, 6559–6568; L.-C. Song, C.-G. Li, J.-H. Ge, Z.-Y. Yang, H.-T. Wang, J. Zhang and Q.-M. Hu, *J. Inorg. Biochem.*, 2008, **102**, 1973–1979; W. Gao, J. Ekström, J. Liu, C. Chen, L. Eriksson, L. Weng, B. Åkermark and L. Sun, *Inorg. Chem.*, 2007, **46**, 1981–1991.
13 D. L. DuBois, C. W. Eigenbrot, J. A. Miedaner, J. C. Smart and R. C. Haltiwanger, *Organometallics*, 1986, **5**, 1405–1411; B. D. Swartz and C. Nataro, *Organometallics*, 2005, **24**, 2447–2451; C. Nataro, A. N. Campbell, M. A. Ferguson, C. D. Incarvito and A. L. Rheingold, *J. Organomet. Chem.*, 2003, **673**, 47–55; G. Pilloni, B. Longato and B. Corain, *J. Organomet. Chem.*, 1991, **420**, 57–65; B. Corain, B. Longato and G. Favero, *Inorg. Chim. Acta*, 1989, **157**, 259–266.
14 G. A. N. Felton, R. S. Glass, D. L. Lichtenberger and D. H. Evans, *Inorg. Chem.*, 2006, **45**, 9181–9184.
15 A. Jablonskyté, J. A. Wright, S. A. Fairhurst, J. N. T. Peck, S. K. Ibrahim, V. S. Oganesyan and C. J. Pickett, *J. Am. Chem. Soc.*, 2011, **133**, 18606–18609.
16 J. C. Gordon and G. J. Kubas, *Organometallics*, 2010, **29**, 4682–4701; C. Greco, G. Zampella, L. Bertini, M. Bruschi, P. Fantucci and L. De Gioia, *Inorg. Chem.*, 2007, **46**, 108–116; C. Greco and L. D. Gioia, *Inorg. Chem.*, 2011, **50**, 6987–6995.
17 J. M. Camara and T. B. Rauchfuss, *J. Am. Chem. Soc.*, 2011, **133**, 8098–8101.
18 J. M. Camara and T. B. Rauchfuss, *Nat. Chem.*, 2012, **4**, 26–30.
19 C. Greco, *Inorg. Chem.*, 2013, **52**, 1901–1908.
20 O. R. Luca and R. H. Crabtree, *Chem. Soc. Rev.*, 2013, **42**, 1440–1459.